Open Access Full Text Article

ORIGINAL RESEARCH

Preparation of Cod Skin Collagen Peptides/Chitosan-Based Temperature-Sensitive Gel and Its Anti-Photoaging Effect in Skin

Songzhi Kong[1], Lijiao Lv[1], Jiaqi Guo[1], Xiaohong Yang[1], Mingneng Liao[1], Tianyang Zhao[1], Haiyang Sun[1], Shuqun Zhang[1], Wenjie Li[2]

[1]School of Chemistry and Environmental Science, Guangdong Ocean University, Zhanjiang, 524088, People's Republic of China; [2]Department of Hematology, Affiliated Hospital of Guangdong Medical University, Zhanjiang, Guangdong, 524001, People's Republic of China

Correspondence: Songzhi Kong, School of Chemistry and Environmental Science, Guangdong Ocean University, 1 Haida Road, Mazhang District, Zhanjiang, 524088, People's Republic of China, Tel +86-759-238-3679, Email kongsongzhi@gdou.edu.cn; Wenjie Li, Department of Hematology, Affiliated Hospital of Guangdong Medical University, People's Avenue, Xiashan District, Zhanjiang, 524001, People's Republic of China, Email dglwj.135@163.com

Background: Photoaging decreases quality of life and increases the risk of skin cancer, underscoring the urgent need to explore natural, high-efficacy, anti-skin photoaging (SP) active substances.

Methods: In this study, a gel (CS/CSCPs/β-GP gel) was prepared using chitosan (CS) and sodium β-glycerophosphate (β-GP) through crosslinking with small molecular CSCPs as the carried drug. We evaluated its structural characteristics and properties. The effect of CS/CSCPs/β-GP gel on the degree of ultraviolet (UV)-induced skin aging of mice was investigated through comparative analysis of skin damage, the integrity of collagen tissues and elastic fibers, levels of reactive oxygen species (ROS) and key inflammatory factors (tumor necrosis factor [TNF]-α and interleukin [IL]-1β, IL-6, and IL-10), and tissue expression of matrix metalloproteinase-3 (MMP-3) after repeated UV irradiation in a nude mice SP model.

Results: The results showed that CS/CSCPs/β-GP gel was successfully prepared and had the desired characteristics. Compared with CSCPs alone, the CS/CSCPs/β-GP gel more evidently improved typical photoaging characteristics on mouse dorsal skin. It also increased the moisture content, causing the skin to become glossy and elastic. Pathological skin analysis revealed that this peptide-carrying gel can effectively inhibit epidermal thickening, reduce tissue inflammatory infiltration, suppress collagen fiber degradation, increase the collagen content, alleviate structural elastic fiber damage, and significantly inhibit abnormal MMP-3 expression. In addition, biochemical analysis showed that the CS/CSCPs/β-GP gel can effectively inhibit the elevated expressions of ROS and key proinflammatory factors (TNF-α, IL-1β, IL-6) in photoaging skin tissues and promote expression of the anti-inflammatory factor IL-10.
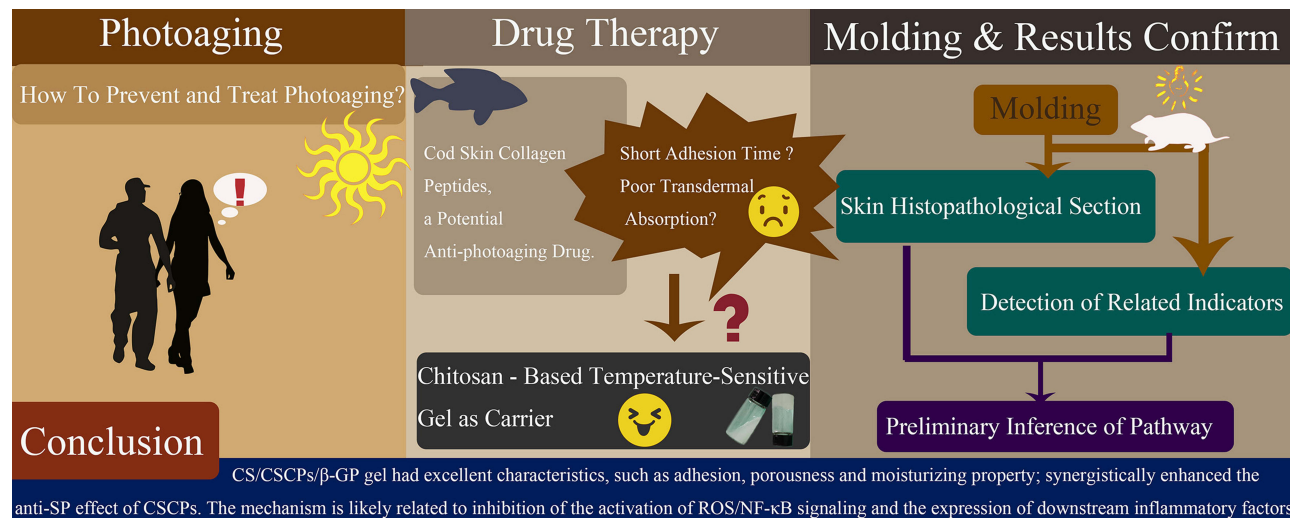
Conclusion: SP can cause many clinical skin diseases, such as solar freckle-like nevus, solar keratosis, cutaneous melanoma, and squamous cell carcinoma. CSCPs are a high-efficacy anti-SP natural active substance and CS/CSCPs/β-GP gel can synergistically enhance the CSCPs' anti-SP effect. The mechanism is likely related to the inhibited activation of ROS/nuclear transcription factor-κB signaling and the expression of downstream inflammatory factors.

Keywords: cod skin collagen peptides, temperature-sensitive gel, chitosan, skin photoaging, ROS/NF-κB

Introduction

Skin aging can be divided into two types: extrinsic or skin photoaging (SP) and intrinsic or inherent aging.[1,2] Different from irreversible inherent skin aging, SP is pathologic and has a clear cause (ie, repeated ultraviolet [UV] irradiation), so this form of skin aging can be prevented and treated.[3] The risk of skin aging in the high-exposure population is 200% greater than in the low-exposure population, and effects of skin aging in the high-exposure population may be observed 10 years earlier. The common clinical manifestations of skin aging in the high-exposure population are skin sagging, thick and deep wrinkles, leather-like appearance, and abnormal pigmentation (eg, lentigines), which further lead to

419

Graphical Abstract

Photoaging

How To Prevent and Treat Photoaging?

Conclusion

Drug Therapy

Cod Skin Collagen Peptides, a Potential Anti-photoaging Drug.

Short Adhesion Time ? Poor Transdermal Absorption?

Chitosan - Based Temperature-Sensitive Gel as Carrier

Molding & Results Confirm

Molding

Skin Histopathological Section

Detection of Related Indicators

Preliminary Inference of Pathway

CS/CSCPs/β-GP gel had excellent characteristics, such as adhesion, porousness and moisturizing property; synergistically enhanced the anti-SP effect of CSCPs. The mechanism is likely related to inhibition of the activation of ROS/NF-κB signaling and the expression of downstream inflammatory factors.

a variety of benign lesions (eg, solar freckles), precancerous lesions (eg, solar keratosis), or malignant tumors (eg, melanoma and squamous-cell carcinoma).[2,3]

Pharmacological and pathological research have shown that the typical appearance of UV-induced SP originates from the degradation of extracellular matrix in the skin mediated by elevated expression of matrix metalloproteinases (MMPs), which is mainly achieved through signaling mediated by reactive oxygen species (ROS).[4] Repeated exposure of skin to UV produces excessive ROS (mainly O_2^-, H_2O_2 and HO_2^-, and OH^-) through interactions with chromophoric groups such as intracellular melanin, uridylic acid, and nucleic acid; these events impair mitochondria function, causing them to produce more ROS during energy metabolism.[5,6] Excessive ROS activates numerous membrane receptors that further influence a series of signal transduction pathways, including nuclear transcription factor-κB (NF-κB) that is a central signaling pathway related to cell apoptosis, inflammatory response, and immune response in the SP process (Figure 1).[5,6] Excess ROS can directly lead to oxidative stress and pro-inflammatory responses in the skin, which cause further imbalance in the inflammatory response.[7–9] Specifically, under repeated and prolonged UV irradiation, the skin tissue produces a large amount of ROS that greatly exceeds the removal capability of endogenous defense systems. The excessive ROS directly cause oxidative stress damage to skin collagen (which contains numerous aliphatic and heterocyclic amino acids, and the side chains of the aliphatic amino acids and the heterocycles of the heterocyclic amino acids are just the sites attacked by ROS)[7,10] and activate IκB kinase (IKK). Activated IKK can phosphorylate IκB, further activating NF-κB. The activated NF-κB molecules enter cell nuclei to induce high expressions of multiple proinflammatory and immunoregulating factors in skin cells, such as interleukin (IL)-1β (IL-1β), IL-6, and tumor necrosis factor (TNF-α) to finally promoting cell necrosis and apoptosis; NF-κB also mediates the transcription of multiple MMPs (especially MMP-1, −3, −9) in skin tissue through binding with the NF-κB sites of their promoters; these proteins degrade extracellular matrix components including collagen, which promotes SP phenomena including skin atrophy and sagging, thick and deep wrinkles, and erythema formation.[11]

SP severely degrades people's appearance and quality of life, and it also has an etiological connection with skin cancer, which seriously endangers human health. For these reasons, SP and relevant issues have always been a research hot spot in the fields of life science, medical science, and dermatology. Within the last several decades, more UV rays reach the ground owing to the destruction of the ozonosphere. Coupled with excessive sunbathing and frequent use of some phototherapeutic devices, the incidence of photoaging has continually increased. The advocacy for natural active
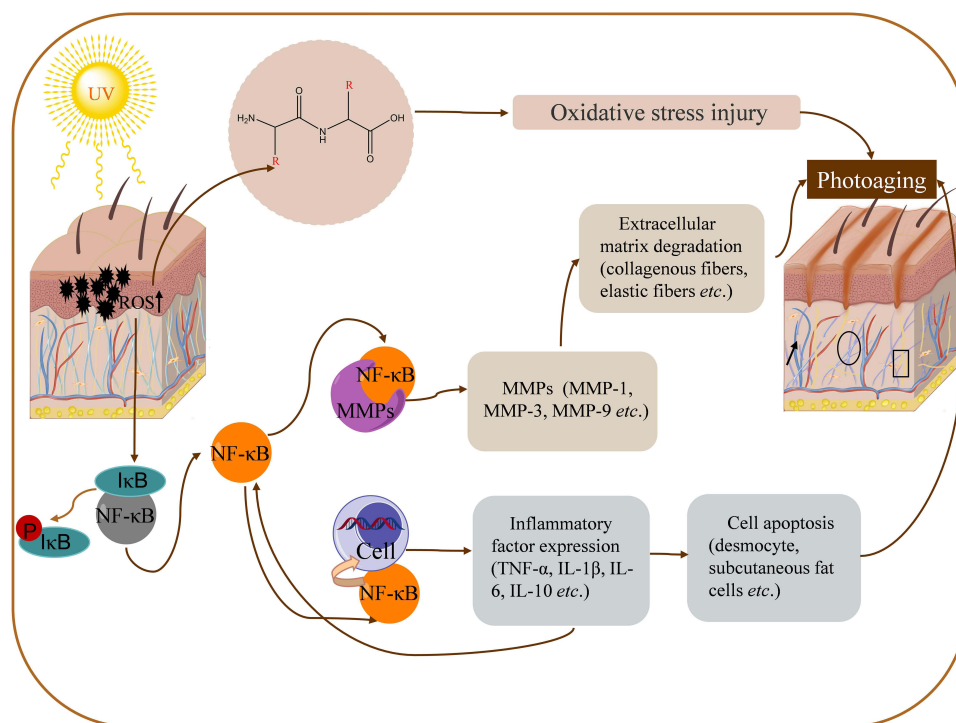
420

Drug Design, Development and Therapy 2023:17

Figure 1 ROS-mediated NF-κB pathway events associated with skin photoaging.
Notes: The black arrow represents an elastic fiber fracture, the black circle represents elastic fiber entanglement, and the black box represents collagen fiber distortion and fracture.

components has led to exploration of the use of natural active substances that are convenient and can prevent and treat SP disease.

Cod are cold-water fish that live in the bottom of the oceans and the middle and lower layers of the deep seas; they are widely distributed throughout the world, rich in collagen, and have extremely high nutritional value. Cod skin is the part with the richest collagen source, accounting for 80% (by dry weight) of total protein content in the cod.[12] Collagen can be decomposed under the action of chemicals, bacteria, or enzymes, and the chains disintegrate and fracture to form products with molecular weights between proteins and amino acids, namely, cod skin collagen peptides (CSCPs).[13] The low temperature and pressure in the deep sea imbue the CSCPs with many excellent properties, such as antioxidation,[14] beauty and skin care,[15] liver injury repair,[16,17] gastric mucosa protection[18] and protection against DNA damage,[19] which are different from the polypeptides obtained from shallow-sea fish, freshwater fish, and terrestrial animals. Since small molecular peptide fragments are more conducive to human absorption and utilization, research on small molecular cod peptides has grown. However, the efforts are mostly concentrated on the preparation, separation, and purification of collagen peptides and the in vitro antioxidation property of collagen peptides; there are relatively few reports on in vivo bioactivity and action mechanisms of collagen peptides.[12,20,21] Some studies have reported that CSCPs have similar structure to collagen in human skin and are rich in moisturizing factors such as aspartic acid, glycine, and serine, which can moisturize skin, smooth out wrinkles, improve elasticity, and repair damaged and aging skin.[22] Others have shown that CSCPs have some anti-SP activity with relatively significant activity at the cellular level.[12,21] However, polypeptides have poor percutaneous absorption and are easily oxidized during adhesion, which has limited deep study on the in vivo anti-SP activity and action mechanisms of CSCPs. Consequently, the present study aimed to overcome the disadvantages of CSCPs for percutaneous absorption with the addition of a carrier and then investigate their in vivo anti-SP effects and explore their mechanisms.

A growing number of studies confirm that UVA can penetrate deeper into the dermis to cause damage of collagen and elastic fibers in the dermis, while UVB can cause erythema, DNA damage, and skin cancer.[23–25] An animal model of SP was established by irradiation of nude mice with UVA and UVB, which is widely used in the research of skin photoaging

diseases because of its similar skin structure with human, ease of handling, and convenient manipulation.[26] Anti-SP drug administration is generally via a local percutaneous route. However, drug permeability is relatively low owing to the barrier effect of the skin cuticle, the strong fluidity of the pure drug solution, and the short time of skin adhesion. Determining how to improve drug adhesion, action time, and percutaneous permeability is therefore important. In recent years, temperature-sensitive gels have exhibited significant advantages in such aspects as sustained drug release and tissue engineering; as a porous, water-absorbent material with good biocompatibility, they are useful drug delivery systems.[27] Among the numerous materials employed for temperature-sensitive gels, chitosan (CS) obtained from shrimp and crab shells is commonly used. CS is one of the few cationic high molecular polymers composed of natural polysaccharides, and it is non-toxic and non-antigenic and has good film-forming property, adhesion property, and biocompatibility. Its positive charges induce electrostatic attraction between the CS and the skin surface with negative charges carried, so the applied layer can more closely contact the skin. Moreover, CS has excellent moisturizing property, so it can effectively improve the hydration degree of cuticle, causing the epidermal cuticle structure to swell and loosen with intercellular space enlarged due to hydration; this reduces the barrier effect and promotes permeation of the carried drug into the skin.[28,29] Based on the above characteristics of chitosan, it was mixed with β-glycerophosphate sodium to make a thermosensitive gel as the matrix, and CSCPs acted as the tested drug.

In this study, CS/CSCPs/β-GP gel was prepared to effectively carry small molecular CSCPs. We validated the effect of the prepared product using an in vivo animal photoaging model and explored its possible action mechanisms to provide experimental bases for the high-value utilization of CSCPs and development of convenient and high-efficacy drug preparations to repair skin photo-damage.

Materials and Methods

Experimental Materials and Reagents

CSCPs were produced by Zhongshi Duqing (Shandong) Biotechnology Co., LTD, detailed information about it will be described in the text. Chitosan (degree of deacetylation 95%, viscosity of 100–200 mpa. s) was purchased from Shanghai Macklin Biopharmaceutical Company. Other reagents were of analytical grade.

Laboratory Animals

Thirty SPF-grade female BALB/c nude mice (42–43 days old, weighing 16–18 g) were provided by the Guangdong Provincial Medical Laboratory Animal Center (production license number, (SCXK (Guangdong) 2018-0002); experimental unit license number for use (SYXK (Guangdong) 2019-0204); animal quality certificate number, 44007200082901). The study was approved by the ethics committee of the animal laboratory of Guangdong Ocean University and strictly followed the "Experimental Animals-Welfare Ethical Review Guidelines" (GB/T 35892-2018). Mice were raised in the Laboratory Animal Center of Guangdong Ocean University; the ambient temperature was 23 ±2°C, the humidity was 55±10%, 12 hours of light and 12 hours of darkness were alternated without any ultraviolet radiation, and food and water were provided ad libitum. All animals were used for subsequent experimental research after 7 days of adaptive feeding.

Sample Preparation

Cod Skin Collagen Peptides (CSCPs)

The CSCP formulation consisted of light yellow dry powder purchased from Zhongshi Duqing Biotech Co., Ltd (Shandong, China). Analysis showed that the molecular weights of the CSCPs were mainly concentrated in the range of <2 kDa (Table 1), and these components accounted for 86.05% of the total weight. A previous study reported that the anti-photoaging activity of collagen enzymolysate with molecular weight <3 kDa is greater than that of high (>10 kDa) and medium molecular (3–5 kDa) enzymolysates.[30,31] This indicates that the CSCPs used in this study have good potential anti-photoaging effects. The contents of several specific amino acids participating in skin repair including Leu, Val, Glu, and Ile were 15.750, 8.443, 6.393, and 6.186 mg/g, respectively (Table 2). Furthermore, the CSCP content of hydrophobic amino acids (Phe, Met, Leu, Val, Ile, and Ala) that can remove relatively many free ions was 58.313mg/g, and that of aromatic

Table 1 CSCP Molecular Weight Distribution

Molecular Weight Range (Da)	Weight Average Molecular Weight (Da)	Proportion (%)
>5000	6279.27	0.29
5000–3000	3918.92	2.91
3000–2000	2468.28	10.75
2000–1000	1442.93	38.01
<1000	571.95	48.04

Table 2 CSCP Amino Acid Composition

Amino Acid	Content (mg/g)	
	Free Amino Acids	Total Amino Acids
Aspartate (Asp)	3.244	6.341
Threonine (Thr)	2.906	5.869
Serine (Ser)	1.279	2.577
Glutamate (Glu)	3.35	6.393
Glycine (Gly)	0.655	1.302
Alanine (Ala)	1.161	2.338
Cystine (Cys)	7.649	15.374
Valine (Val)	4.211	8.443
Methionine (Met)	1.363	2.669
Isoleucine (Ile)	3.142	6.186
Leucine (Leu)	7.917	15.750
Tyrosine (Tyr)	10.732	21.524
Phenylalanine (Phe)	11.758	22.927
Histidine (His)	0.577	1.199
Lysine (Lys)	0.995	1.972
Arginine (Arg)	0.190	0.382
Total	61.129	121.246

amino acid residues (Tyr) with a strong antioxidation effect was 21.524mg/g (Table 2), indicating that the CSCPs have potential antioxidation damage activity.[32,33] These potentials are why we selected the CSCPs as the experimental object.

Preparation of Temperature-Sensitive Gel

First, 2.0 g of CS powder was accurately weighed and then dissolved in 100 mL of 1% acetic acid solution. Magnetic stirring was conducted for 4 hours at room temperature so the CS was completely dissolved. Then, 2.0 g of CSCPs powder was added, and stirring was conducted to dissolve the CSCPs powder, generating solution A. Separately, 6.0 g of β-GP powder was accurately weighed and then dissolved in 10 mL of ultrapure water. Shaking was conducted so that the β-GP powder was completely dissolved, generating solution B. The prepared solution B was added into solution A drop by drop at a ratio of 3:7 (B:A), and stirring was conducted at room temperature throughout the process. After the additions were complete, the solution was stirred for 15 minutes to generate the temperature-sensitive gel solution, which was placed in a thermostatic water bath (37 °C), to yield CS/CSCPs/β-GP gel test samples. The preparation process is shown in Figure 2A.

The preparation process of the blank gel was similar to the above preparation process for the test sample, but CSCPs were omitted to yield CS/β-GP gel.
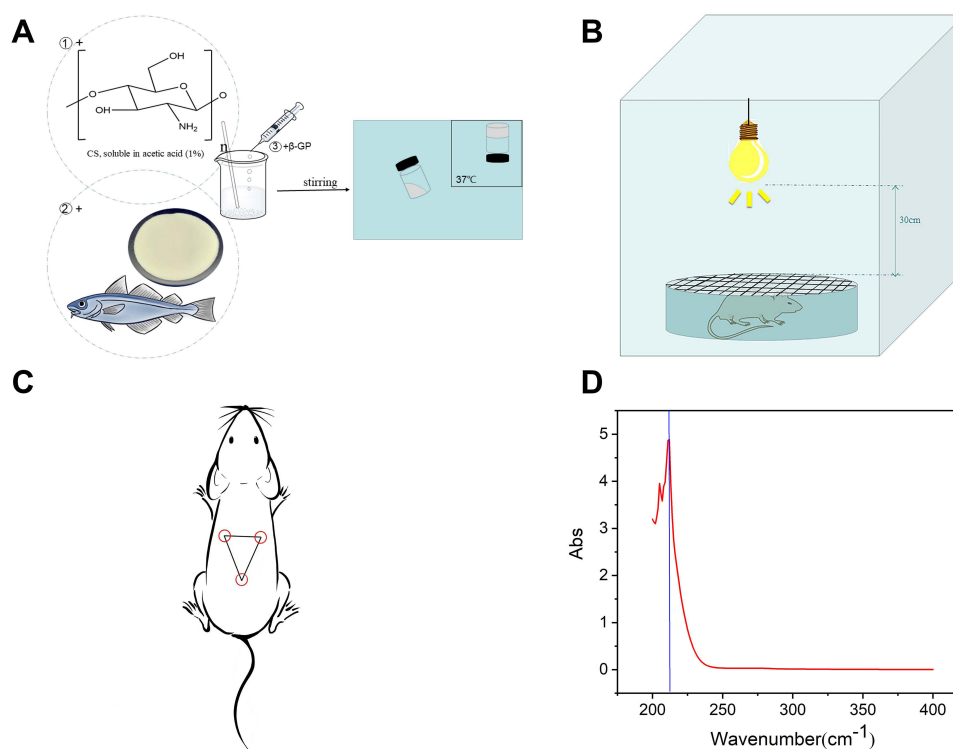
Figure 2 CS/CSCPs/β-GP gel preparation (**A**). Schematic depicting the UV radiation set up for modeling (**B**). Dorsal skin analysis area of moisture determination (**C**) and UV spectra of CSCPs (**D**).

Sample Characterization

UV Spectra

A measured amount of CSCPs powder was used to prepare 20 mg/mL solution with ultrapure water. The UV absorption of this solution was tested with a UV spectrophotometer (756S, Lengguang, Shanghai, China) with a scanning wavelength range of 200–400 nm and a scanning speed of 100 nm/min.

Macroscopic Observation and pH Measurement of Samples

A measured amount of temperature-sensitive gel solution was placed in a spiral mouth bottle, and the morphological changes were observed. A pH meter (SX5150; Sanxin, Shanghai, China) was used to detect the pH of the sample, and the average value was taken three times.

Determination of Gelling Time and Temperature

A measured amount of temperature-sensitive gel solution was placed in a 3-mL spiral mouth bottle, which was then placed into a thermostatic water bath (37 °C). When the fluidity began to decrease, the gel status was observed and recorded once every 30 seconds. The recorded gelling time was the time lapsed when the mixture in the bottle stopped flowing when the spiral mouth bottle was inverted.

Rheological analysis of the temperature-sensitive gel solution was carried out with a Haake rheometer (MARSIII, HAAKE, Vreden, Germany), with a cone/plate combination of C35/1: φ=35 mm and angle=1° as the measuring system. One (1) mL of gel solution sample was put into the rheometer, and the rheological property of the sample was measured at a constant frequency of 1 Hz and a heating rate of 1 °C/min in the temperature range of 20–60 °C. Changes in the storage modulus G' (Pa) and loss modulus G'' (Pa) were recorded as functions of temperature to evaluate the sample's gelling temperature.[34] The temperature was kept constant at 37 °C and measured over a time range of 0–30 min to collect data. The sol–gel transition time is the time at the intersection of G'(Pa) and G''(Pa).

424

Drug Design, Development and Therapy 2023:17

Scanning Electron Microscopy

The CS/CSCPs/β-GP gel test sample dried by lyophilization was metal sprayed to prepare a specimen, which was then placed under a scanning electron microscope (SEM; Tescan, Brno, Czech Republic) and observed and photographed at an accelerating voltage of 10 kV.

Test of Moisturizing Property

A small CS/CSCPs/β-GP gel test sample was weighed and placed into a beaker. Weighing was carried out once every 10 minutes at 37 °C, and the mass change of sample was recorded. The initial mass of the sample under test was recorded as m_0, and the sample mass after n minutes was recorded as m_n. The moisturizing rate (%) was calculated as $m_n/m_0 \times 100\%$.

Determination of Infrared Spectra

The CS, CSCPs, β-GP, CS/β-GP gel, CS/CSCPs/β-GP gel, and KBr in a dry powder state were compressed into tablets, and then the infrared spectra were determined with a Fourier transform infrared spectrometer (Spectrum 100, Perkin Elmer, Waltham, MA, USA) with a scanning wavenumber range of 4000–400 cm^{-1} and a resolution of 4 cm^{-1}.

Cumulative Drug Release Rate

CS/CSCPs/β-GP gel was put into a dialysis bag for dialysis under magnetic agitation. After a predetermined time, 1.5 mL of sample solution was measured with a UV spectrophotometer, and CSCPs content determined at 212 nm was calculated by the CSCPs standard curve (y = 0.0779x + 0.3191, R^2 = 0.9991), and 1.5 mL release medium (normal saline) was added at the same time to keep the volume unchanged. The measured values were averaged three times, and the cumulative drug release rate was calculated according to the following formula:

$$Q = \frac{V_e \sum_1^{n-1} C_i + V_0 C_n}{m_{(drug)}} \times 100\%$$

Q: cumulative drug release rate (%); V_e: displacement volume of release medium (mL); V_0: total volume of release medium (mL); C_i: concentration of the released medium at the i displacement sampling (mg/mL); m(drug): the total weight of the drug contained in the gel (mg); n: number of times to replace release medium.

Animal Grouping and Modeling

Grouping

After acclimatization for 7 days, 30 nude mice were randomly divided into 5 groups (n = 6 each) as shown in Table 3. The experimental setup is shown in Figure 2B.

Modeling and Drug Administration

Modeling was conducted with a UV lamp (Ultra-vitalux 300W, Osram, Munich, Germany, λ 365–450 nm, UVA 15%, UVB 3%) to irradiate the dorsal skin of nude mice. The specific methods were described in a previous publication with slight modifications.[35] Briefly, UV radiation treatment was performed daily in this study, while mice were exposed to UV radiation five times weekly (except Thursday and Sunday) in the referenced literature.

Table 3 Experimental Animal Groups

Group	Dosing
Control (C)	No UV irradiation or drug was given.
Model (M)	The dorsal skin of mice was irradiated with UV light for 1–4 min/d, but no drug in any dosage form was given.
Blank gel (J)	Blank gel was applied at an amount of 0.2 mL/d after irradiation.
CSCPs (T)	CSCP solution (0.2 mL/d) was applied after irradiation.
CS/CSCPs/β-GP gel (T-J)	Self-made thermosensitive gel was applied at an amount of 0.3 mL/d after irradiation.

Skin Status Evaluation

At the end of week 8, moisture determination was carried out on three areas of back skin for each mouse in all groups with a skin moisture meter (Corneometer@CM825, C+K Company, Köln, Germany) (Figure 2C), and the obtained mean value represented the skin moisture level. The irradiated back skin was photographed, and the macroscopic characteristics were observed. The skin was evaluated based on the SP criteria proposed by Bissett et al[36] (see Box 1 for the specific evaluation criteria).

Tissue Staining Analysis

The back of each mouse was cleaned 24 hours after the final drug administration. The animals were then killed by cervical dislocation, and the whole layer of skin at the experimental site was quickly removed. The connective tissue and subcutaneous fat were peeled off, and a small piece ($\sim$0.5×1.0 cm^2) of central dorsal skin tissue was rapidly dissected. The skin tissue was fixed for 48 hours in 4% paraformaldehyde and then conventionally dehydrated. After paraffin embedding, the skin tissue was cut into 5-μm-thick sections.

The above sections were subjected to hematoxylin-eosin (H&E), resorcinol, Masson staining, and immunohistochemistry, then observed and photographed under an optical microscope. The images were analyzed with Image-Pro Plus 6.0 software (Media Cybernetics, Rockville, MD, USA), including quantitative assessment of epidermal hyperplasia and measurement of collagen level in three visual fields. The collagen ratio (%) was calculated as Area of blue area/Total area of dermis layer × 100%, with the mean value representing the collagen level in the corresponding skin. MMP-3 expression in each section was assessed in at least three 200× visual fields that were randomly selected for photographing, and each image was analyzed to obtain the positive average optic density (AOD), with the mean value representing the MMP-3 expression level in the skin.

Evaluation of Levels of ROS and Inflammatory Factors

The remaining fresh skin tissue ($\sim$0.3 g/mouse) collected as described above was rapidly rinsed twice with pre-cooled normal saline, wiped with filter paper, and weighed. A corresponding volume of normal saline (4 °C) based on a ratio (1:9) of tissue mass (g) to normal saline volume (mL) was added, and the mixture was put into a freeze grinder to be ground into 10% tissue solution. The tissue solution was freeze separated (4 °C, 2500 rpm, 10 min), and the supernatant (skin tissue homogenate) was collected for testing the following biochemical indices.

Appropriate amounts of the above prepared tissue homogenate were measured for expression levels of ROS, TNF-α, and key inflammatory factors (IL-1β, IL-6, IL-10) strictly according to the manufacturer instructions for corresponding enzyme-linked immunosorbent assay kits.

Statistical Analysis

Statistical processing was carried out with SPSS 26.0 software (IBM Corp., Armonk, NY, USA). The results in each group are expressed as the mean ± standard deviation (SD). Shapiro–Wilk test and QQ plots were used to assess the normal distribution of data. Differences between groups were compared using one-way analyses of variance, and $p <$ 0.05 was considered significantly different. The LSD test was used when the variance was homogeneous, while the Dunnett's T3 test was chosen when the variance was non-homogeneous.

Box 1 Photoaging Progression Evaluation

Grade	Apparent Characteristics
0	No wrinkles or sagging; normal skin texture all over the body
1	Normal skin texture
2	Normal skin texture disappears
3	Shallow wrinkles
4	Few deep wrinkles and mild sagging
5	More deep wrinkles, severe wrinkles
6	Occurrence of tumors and lesions

Results

Sample Characterization Results

UV Spectra of CSCPs

As shown in Figure 2D, the CSCPs had some absorption effect for 200–400 nm UV rays; the maximum absorption peak was at 200–215 nm, with weak absorption in other wavelength ranges. Consequently, the drug was locally applied onto the skin after each UV irradiation to study the treatment efficacy. This approach avoided physical absorption of UV rays by the drug solution, which might impact the efficacy results.

Macroscopic Characterization and pH of CS/CSCPs/β-GP Gel

At room temperature, the temperature-sensitive gel solution was a milky liquid that could flow (Figure 3A i). At temperatures >36 °C, it was visible to the naked eye that the solution turned from liquid into jelly-like material, forming CS/CSCPs/β-GP gel (Figure 3A ii). The pH value of the sample was 6.43 ± 0.01, which was close to the pH of skin (5.0–7.0), indicating that it would not affect the acid-base balance of the skin.

SEM Analysis of CS/CSCPs/β-GP Gel Microstructure

The microstructure of the CS/CSCPs/β-GP gel was observed and analyzed with an SEM. As shown in Figure 3B, both the CS/β-GP and CS/CSCPs/β-GP gels prepared in this study exhibited three-dimensional reticular porous structures. Compared with the blank gel (Figure 3B i), the CS/CSCPs/β-GP gel (Figure 3B ii and 3B iii) had a more uniform porous structure with relatively deep pores but a rougher surface, likely due to the added CSCPs.

Gelling Time and Temperature of CS/CSCPs/β-GP Gel

The prepared temperature-sensitive gel was liquid that flowed at room temperature (25 ± 2 °C), and the liquid turned into gel at 36–37 °C (Figure 3A i and 3A ii). The gelling time was tested using the reversing method and was 120 ± 10s. The time for gel formation was relatively short, suggesting that it is favorable for drug administration through dermal application.

The rheological properties of the CS/CSCPs/β-GP gel are shown in Figure 3C. The intersection of storage modulus G' and loss modulus G'' corresponded to 36.3 °C (Figure 3C i), at which the sample transitions from the sol state into the gel state, so the gelling temperature of the CS/CSCPs/β-GP gel was 36.3 °C. The cross point of G' and G'' corresponds to the gelation time of the sol-gel transition (Figure 3C ii). The gelation time of CS/CSCPs/β-GP at 37 °C was 8.5 min. Compared to detection by the human eye, this was a longer gelation time. This may have been influenced by different test methods, as the reversing method can be subjective depending on the observer.

Moisturizing Property of CS/CSCPs/β-GP Gel

The change in moisturizing degree of the CS/CSCPs/β-GP gel with time at 37 °C was shown in Figure 3D. As the time increased, the moisturizing rate exhibited a descending trend. When the time reached ~330 min, the moisturizing rate was still >50%, indicating that the CS/CSCPs/β-GP gel had a good moisturizing effect.

Comparative Analysis of Infrared Absorption Spectra of Test Samples

The infrared absorption spectra of all samples (Figure 3E) indicated that compared with CS, both the CS/β-GP and CS/CSCPs/β-GP gels had red shift phenomena of the absorption peaks near 3425 cm^{-1}, with relatively flat peaks. This may be caused by the superposition between the hydroxyl group in the CS and that in the β-GP or by the hydrogen bond formed through the interaction between the amino group in the CS chain and the hydroxyl group in the β-GP. The absorption peaks at 1655 cm^{-1} and 1592 cm^{-1} of the CS are the characteristic absorption peaks of amide I (stretching vibration of C=O) and amide II (bending vibration of N-H), respectively. After gelling, these two absorption peaks had red shift phenomena with characteristic absorption weakening. This may be caused by hydrogen bonds between the CS and β-GP, indicating that the CS-based temperature-sensitive gel was formed through physical crosslinking. In addition, other absorption peaks in the spectra were similar between the CS/CSCPs/β-GP and CS/β-GP gels, so we infer that the CSCPs were added into the blank gel through simple physical mixing, without a chemical reaction occurring.
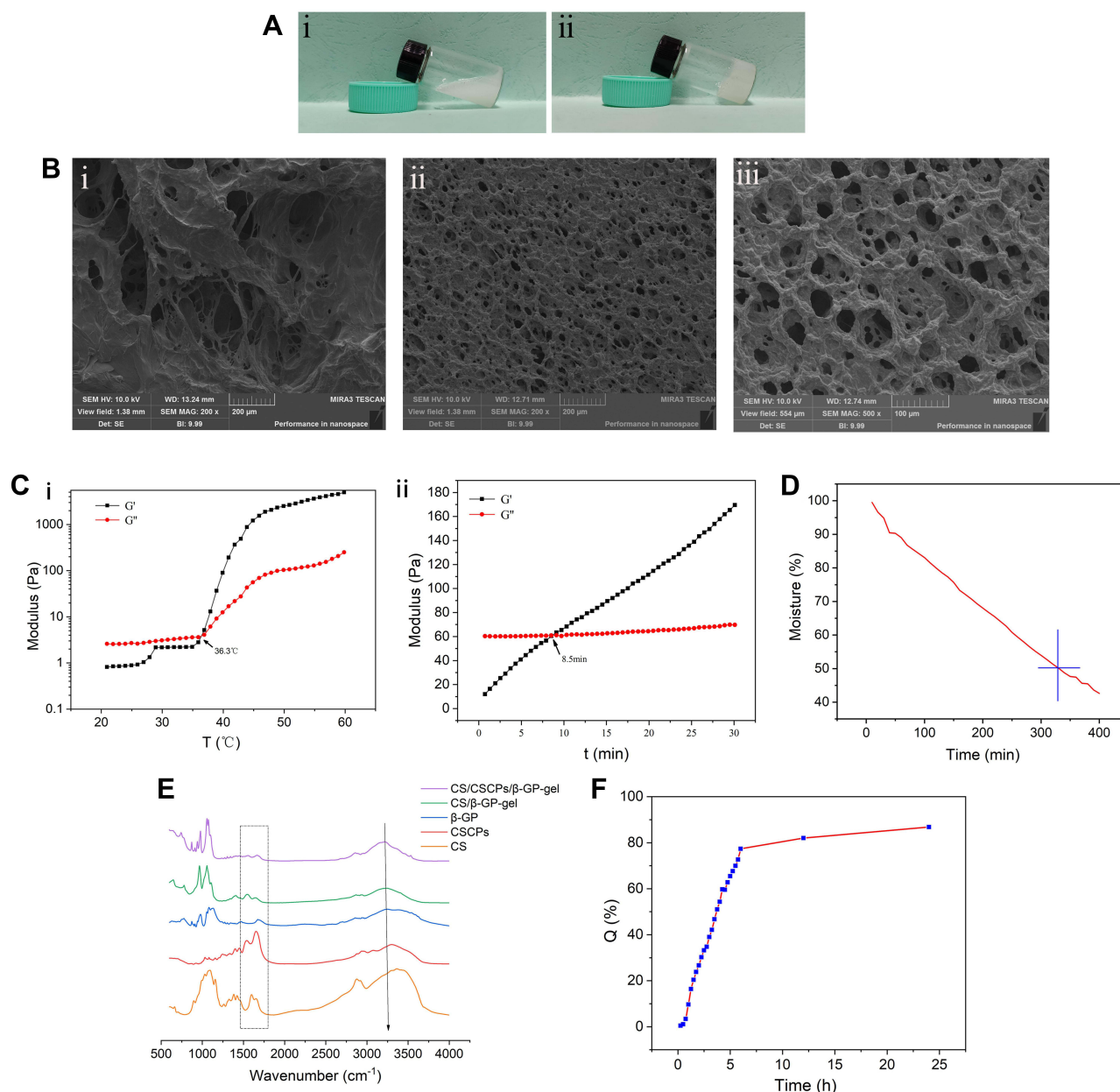
Figure 3 Images of the temperature-sensitive sol (i) and gel (ii) states (**A**). The electronic spectra of CS/β-GP gel (i) and CS/CSCPs/β-GP gel (ii, iii) (**B**). Storage modulus (G′) and loss modulus (G″) of the sample: CS/CSCPs/β-GP gel as a function of temperature (i); G′ and G″ of the sample: CS/CSCPs/β-GP gel as a function of time (ii) (**C**). Moisture level of the temperature-sensitive gel over time (**D**) and FTIR spectra of CS/CSCPs/β-GP gel, CS/β-GP gel, β-GP, CSCPs and CS (**E**). Cumulative drug release rate of CS/CSCPs/β-GP gel (**F**).

Cumulative Drug Release Rate

As shown in Figure 3F, the release behavior of CSCPs showed a nearly linear continuous release over 0–6 hours. After that, the release speed decreased, but the release process lasted for 24 hours, and the cumulative drug release rate was 86.83%, indicating that most CSCPs could be released from CS/CSCPs/β-GP. These results demonstrate that CS/CSCPs/β-GP showed desirable sustained-release effects, which could prevent rapid loss of CSCPs.

Improvement Effect of CSCPs on Irradiated Mouse Skin

The macroscopic effects of 8 consecutive weeks of UV irradiation to the back skin of the mice in all groups are shown in Figure 4. Compared with the nude mice in group C, which had moisturized and smooth skin with only local shallow
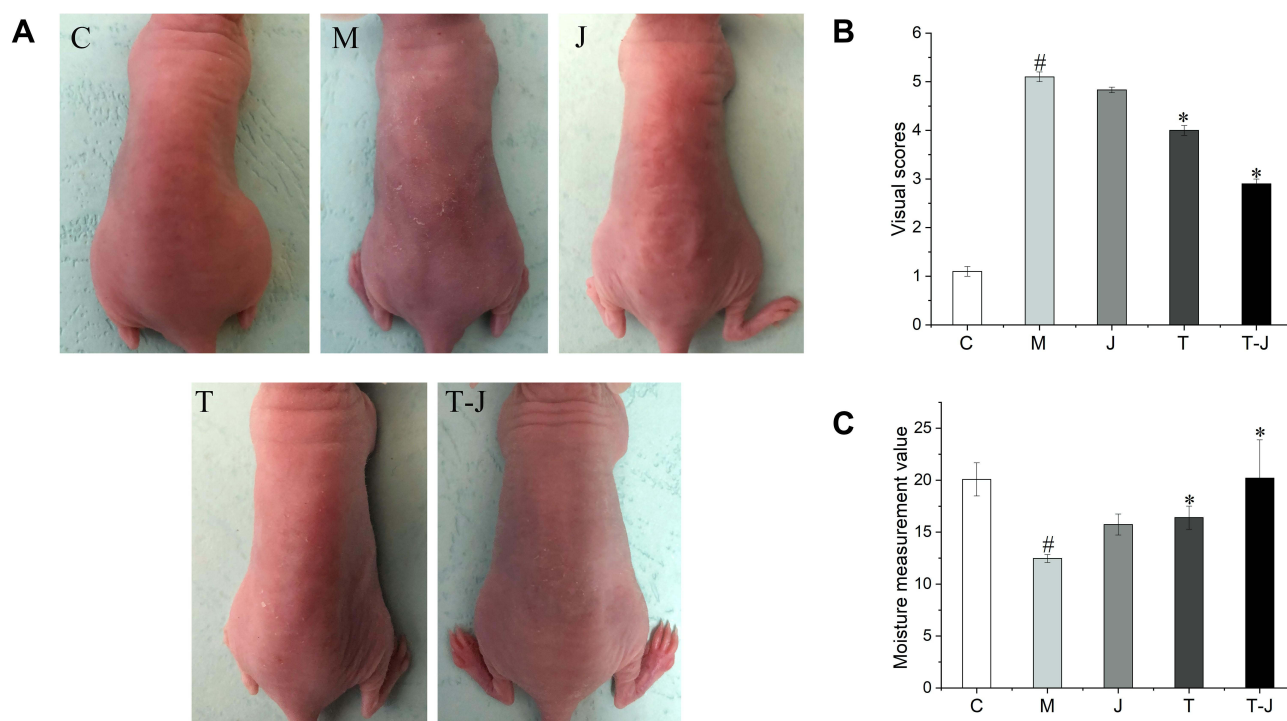
Figure 4 CS/CSCPs/β-GP gel prevents UV-induced macroscopic changes in mouse skin (**A**). Visual scores of skin on the dorsal surface of mice among the different experimental groups (**B**) and valuation of the moisture content of CS/CSCPs/β-GP gel (**C**). Data are shown as means ($\bar{x}$± SD, n = 6). #p < 0.05 vs group C; *p < 0.05 vs group M.

wrinkles, the back skin of the mice in group M was dry with sagging, darkening, deep wrinkles, and even a leather-like appearance and slight flesh-colored lesions, which are typical characteristics of photoaging skin. The macroscopic evaluation score and moisture content in group M were significantly different (p < 0.05) from those in group C, indicating successful SP model generation. The dorsal skin appearance of the mice in group J was slightly better than that in group M, but it still showed wrinkling, sagging, skin damage, and a leather-like appearance. The macroscopic evaluation score and moisture content were not significantly different between these two groups, indicating that the blank gel does not improve the characteristics of photoaging skin. Compared with group M, the following were observed in mice in group T: wrinkle shallowing, skin damage reduction, reduced leather-like appearance, and significantly higher skin moisture content (p < 0.05). The macroscopic evaluation score was also significantly lower than in group M (p < 0.05), indicating that the CSCPs have some photoaging skin repair effect. Compared with the mice in group M, those in group T-J had smooth, moisturized, glossy skin with slight erythema and shallow wrinkles. The skin moisture content increased significantly (p < 0.05), while the macroscopic evaluation score was significantly lower than in group M (p < 0.05). Compared with the mice in group T, those in group T-J exhibited even more evident skin improvement and higher moisture content, indicating that continuous local application of CS/CSCPs/β-GP gel can help skin resist macroscopic damage and moisture loss. Since the CSCPs are usually liquid, some run-off may occur after dermal application, thus weakening the effect. When incorporated into gel, CSCPs are retained longer on the skin with extended action time, so the effect is even more evident.

CSCP Improvement of UV-Induced Skin Histological Damage and Abnormal Epidermal Hyperplasia

As shown in Figure 5A, the skin of the mice in group C had clearly visible layers and complete structure. The epidermis was relatively thin with uniform thickness, the epidermis and dermis were closely connected in a wave shape with a clear boundary, and the tightly interwoven collagen bundles in the dermis were also clearly visible. Skin from mice in the UV irradiation group (group M) exhibited typical pathological characteristics of photoaging, such as irregular thickening of
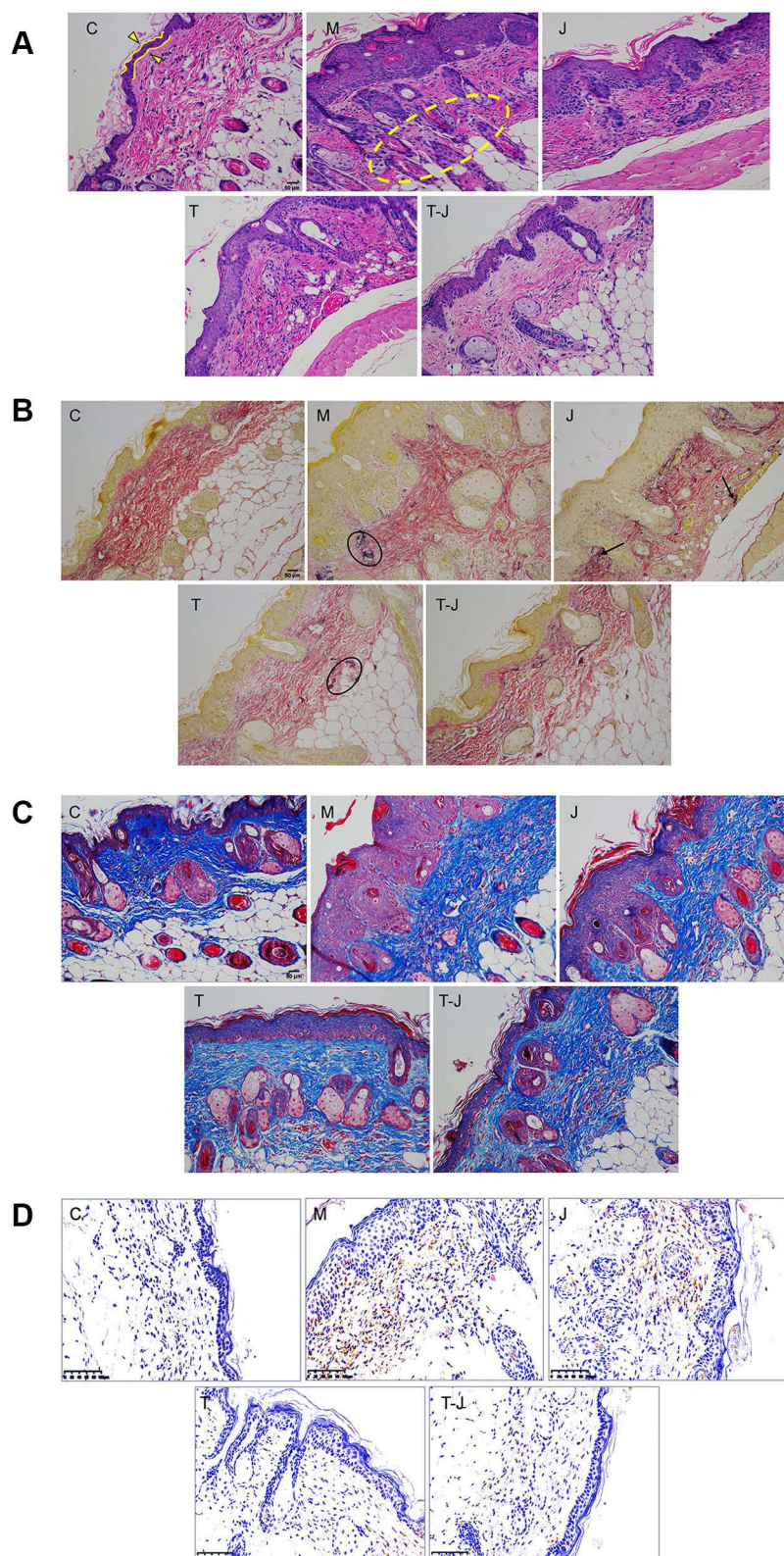
Figure 5 Histological changes of mouse skin (200×) (**A**). Elastic fibers in mouse skin tissue (200×) (**B**). Masson trichrome staining of mouse skin (200×) (**C**). Immunohistochemical staining of mouse skin tissue (200×) (**D**).

Notes: Epidermal thickness (excluding cuticle thickness) is shown with yellow lines, and inflammatory cell infiltration is indicated by the yellow circle (**A**); the circles in black represent collagen fiber aggregation and tangling, and arrows indicate broken collagen fibers (**B**).

the epidermis layer, a flattening of the boundary between the epidermis and dermis, sparse and disorderly collagen fibers, and even inflammatory infiltration in the dermis and subcutaneous tissue. Collectively, these effects indicated that the photoaging model was successfully established. The skin status of mice in group J was relatively similar to that of the mice in group M, with relatively thick epidermis and dermis layers that were not quite regular, and the inflammatory cell infiltration phenomenon was also seen, indicating that the blank gel does not evidently improve pathological changes in photoaged skin. Compared with group M, mice in the CSCPs treatment group T had more complete skin structure, the epidermis was slightly thickened and more uniform, and there was a clear boundary with the dermis, indicating that the CSCPs had some improvement effect on photoaged skin. In group T-J, the skin had complete structure, the epidermis was relatively thin with clear and regular layers, the boundary between epidermis and dermis was clear and in a wave shape, and there was no evidence of inflammatory cell infiltration, indicating that the CS/CSCPs/β-GP gel has a good anti-SP effect.

Irregular thickening of the epidermis layer (ie, epidermal hyperplasia) is normally used as a parameter to evaluate inflammation and wrinkles formed in SP,[8] so we measured the epidermis thickness of each mouse (mean epidermis thickness of three randomly selected areas measured in each H&E-stained pathological section). The results are shown in Figure 6A. Compared with group C, the dorsal skin in group M showed a significant increase in epidermis thickness ($p < 0.05$), indicating successful establishment of a murine SP model. Compared with group M, group J had a non-significant decrease in epidermis thickness. Such abnormal epidermis hyperplasia caused by chronic UV irradiation was evidently inhibited by locally applied CSCPs and CS/CSCPs/β-GP gel ($p < 0.05$ vs group M), and the Improvement effect of the CS/CSCPs/β-GP gel was more significant than that of the CSCPs.

CSCP Inhibition of UV-Induced Damage to Skin Elastic Fibers

Elastic fibers account for a very small part in the dry weight of skin, but they are critical to maintaining an elastic and smooth structures. When elastic fibers are damaged or broken, the reticular structure of the dermis layer is directly destroyed, which causes the skin to wrinkle and sag.[37] In this study, the elastic fiber state in the dermis layer was observed using the resorcinol staining method, and the results are shown in Figure 5B. In the normal group (group C), the elastic fibers in the dermis layer showed orderly orientation and were relatively complete, and the purplish-red filamentous elastic fibers were reticularly interwoven, with only rare pileup and fracture phenomena. In group M, the elastic fibers thickened, fractured, and were distorted. Some of them were aggregated, entangled, and disorderly, indicating that UV stimulation can damage the elastic fibers in the skin dermis layer of the mice and destroy their reticular structure, which leads to macroscopic sagging and drooping of photoaging skin. The state of fibers in the dermis layer of group J was similar to that in group M, without evident improvement. In group T, the elastic fibers were arranged relatively orderly, and some of them still had the entanglement phenomenon. In group T-J, the elastic fibers were arranged relatively orderly in a reticular structure seen, but aggregation, fracture, and entanglement phenomena were occasionally seen. Collectively, these findings indicate that compared with directly applied CSCPs, the CS/CSCPs/β-GP gel prepared in this experiment had a better effect to resist damage to elastic fibers.

CSCP Inhibition of UV-Induced Degradation of Skin Collagen

Previous studies demonstrated that collagen degradation caused by repeated UV irradiation is the direct cause of such typical SP characteristics as sagging and wrinkling,[8] so we investigated the distribution, morphology, and relative content (ie, collagen ratio) of collagen fibers in the dermis of photoaging skin of the mice using the Masson staining method. The results are shown in Figure 5C. In the normal group (group C), collagen fibers in the dermis were fascicular (bright blue) and were orderly arranged and densely and distributed in a uniform fashion. In the model group (group M), the collagen fiber bundles in the dermis exhibited distortion and fracture phenomena and abnormal aggregation, and the relative collagen fiber content was evidently lower than in the normal control group ($p < 0.05$, Figures 5C and 6B). Compared with group M, group J did not exhibit evident improvement in collagen fiber distribution or arrangement, and the collagen ratio was not increased, indicating that the blank gel failed to help skin resist collagen degradation induced by repeated UV irradiation and the subsequent sagging and disorder arrangement. Conversely, local administration of CSCPs and CS/CSCPs/β-GP gel alleviated UV-induced collagen fiber degradation, normalized the morphology and
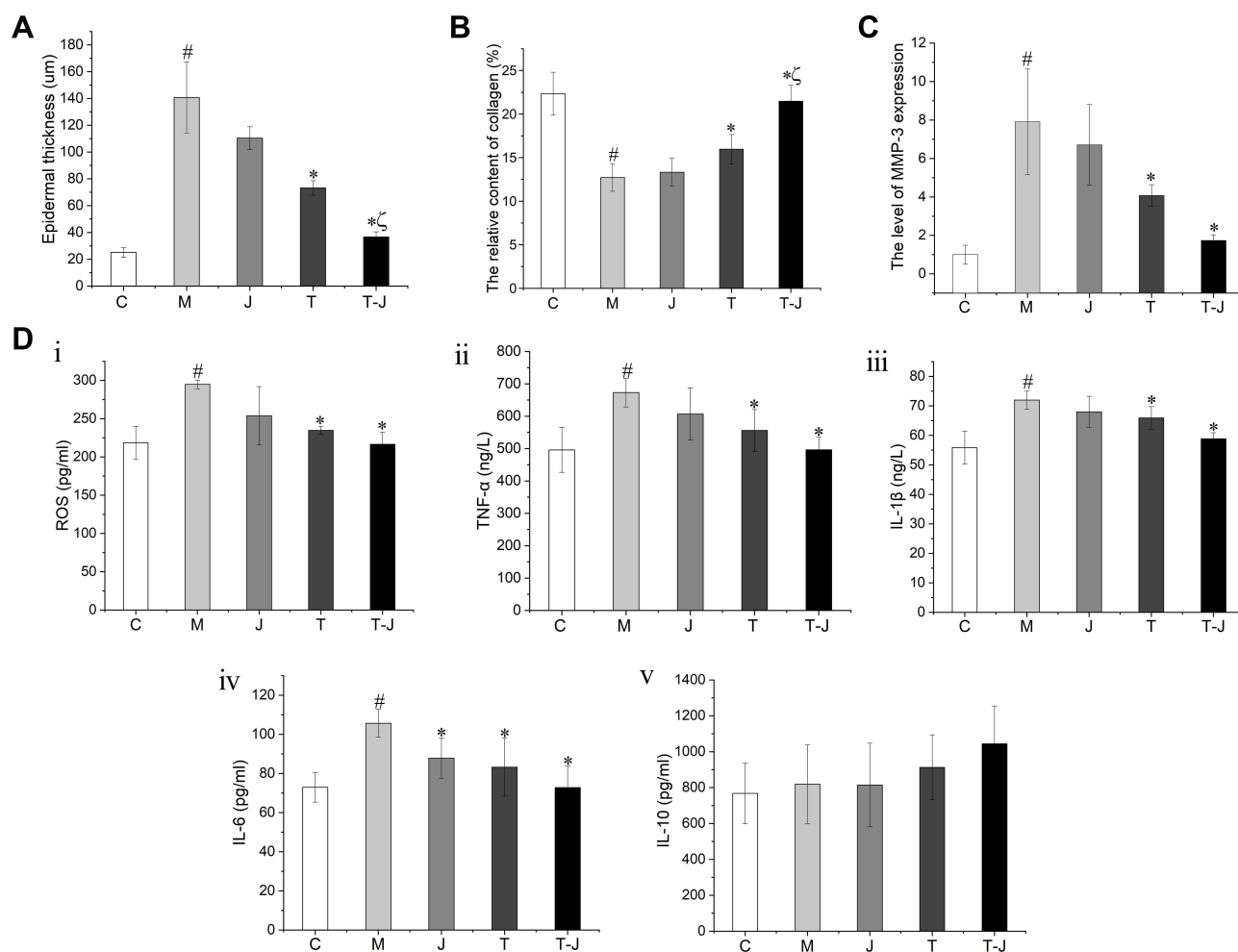
Figure 6 Epidermal thickness by H&E staining (**A**). The relative collagen content in mouse skins (**B**). MMP-3 levels of in PA-affected skin tissue (**C**). Levels of ROS (i) and the inflammatory factors TNF-α (ii), IL-1β (iii), IL-6 (iv), and IL-10 (v) in each group (**D**). Data are shown as means ($\bar{x}$± SD, n = 6). #$p < 0.05$ vs group C; *$p < 0.05$ vs group M; ζ$p < 0.05$ vs group T.

arrangement distribution of collagen fiber bundles, and evidently increased the relative content of collagen relative to the model group ($p < 0.05$ vs group M). In particular, the effect of the CS/CSCPs/β-GP gel was more prominent ($p < 0.05$ vs group T), indicating that local administration of the CS/CSCPs/β-GP gel prepared in this experiment effectively inhibited UV-induced degradation of collagen fibers in the dermis and prevented skin sagging and wrinkling.

CSCP Inhibition of UV-Induced MMP-3 Expression

UV-induced SP mainly originates from skin collagen degradation caused by excessive MMP expression. Among the members of the large MMP family, MMP-3 has broader substrate specificity and degrades multiple types of collagen fibers (eg, types III and V) by itself; together with MMP-1, most extracellular matrix components in the dermis can be degraded, so MMP-3 is one of the root causes of typical SP appearance characteristics.[38,39] Consequently, we measured the expression level of MMP-3 in mouse skin tissue, and the results are shown in Figures 5D and 6C. Compared with group C, skin tissue in group M had more yellowish-brown particles, and the expression level of MMP-3 distinctly increased. The expression level in the skin of the mice in group J was similar to that in group M. Compared with group M, the groups with locally administered CSCPs and CS/CSCPs/β-GP gel exhibited apparent decreases in the number of yellowish-brown particles and lower MMP-3 expression ($p < 0.05$ vs group M); this inhibition effect was more evident in the group treated with CS/CSCPs/β-GP gel than in mice treated with CSCPs.

Influence of CSCPs on the Expression of Key ROS/NF-κB Signaling Molecules in Skin Tissue

Repeated UV irradiation can induce skin tissue to continuously produce excessive ROS, which can activate the NF-κB pathway, inducing the expression of multiple inflammatory factors, and the subsequent persistent inflammatory response plays an important role in SP pathogenesis.[40,41] As shown in Figure 6D, the contents of ROS, TNF-α, IL-1β, and IL-6 in the skin of model group mice receiving UV irradiation were all higher than those in the normal control group ($p < 0.05$). IL-10 levels were somewhat increased in the model group compared to the normal group, albeit not significantly ($p > 0.05$). All of the above indices in group J were similar to those in group M. However, compared with the model group, the group with CSCPs applied after each irradiation showed a lower degree UV-induced abnormal changes, and the group treated with CS/CSCPs/β-GP gel exhibited significant decreases in the levels of the above proinflammatory factors and ROS and an evident increase in IL-10. By promoting the balance between pro- and anti-inflammatory factors, CSCPs can effectively inhibit the development of skin inflammation.

Discussion

SP phenomena become evident in people with skin subjected to chronic UV irradiation (eg, often performing outdoor activities). It is well known that UV rays are the core factor causing SP, and they include short-wave UV (UVC, wavelengths of 200–290 nm), medium-wave UV (UVB, wavelengths of 290–320 nm), and long-wave UV (UVA, wavelengths of 320–400 nm). The bioactivity of UVB is much stronger than that of UVA, and UVB is normally regarded as the main cause of damage to skin. However, recent studies have shown that UVA can also cause skin damage since it has far higher penetration capability than UVB and can more easily reach the dermis layer, causing more serious skin changes than those caused by UVB.[42,43] Therefore, the joint effects of UVA and UVB promote skin aging. Accordingly, 15% UVA + 3% UVB was selected as the light source to simulate photoaging in nude mice. In addition, the constant worsening of environmental conditions and ozonosphere thinning have increased the amount of UVC that reaches human skin, so its influence on SP cannot be ignored. Indeed, UVC can also evidently damage skin cells.[44,45] Based on CSCP's absorption status in the range of UV 200–400 nm (mainly concentrated in short wavelength range, with a maximum absorption peak in the range of 200–215 nm), these molecules should be further studied for the development of physical sunscreen products including UV protection/resistant products (especially for short-wave UV).

With greater awareness about health and environmental protection, people are more inclined to use natural active substances rather than artificial products to improve the skin state. Identifying natural active substances to effectively prevent and/or treat photoaging has long been a research hot spot in the fields of life science, medical science, and dermatology.[9,46] Owing to the low temperature and pressure in the deep sea, the active components in the skin of organisms living in this environment typically have many excellent properties,[14–19] which are unique active components compared to those carried by shallow-sea and terrestrial creatures. Consequently, the anti-SP activity and possible action mechanisms of deep-sea CSCPs were investigated. Previous studies demonstrated that many marine-derived fish skin polypeptides can exert antioxidant effects.[47–51] Here we show that CSCPs can clear excessive ROS and regulate inflammatory factor expression, which is consistent with reports of anti-oxidation and anti-inflammatory effects of CSCPs.[14–19,52] The small polypeptides used in this study had molecular weights mainly concentrated in the range of <2 kDa, and it is reported that the anti-photoaging activity of collagen enzymolysate with low molecular weight is greater than that of medium and high enzymolysates.[30,31,48,53] Another report proposed that the skin repair effect for collagen peptides is related to the polypeptide's amino acid composition, and several specific amino acids (ie, Arg, Glu, Val, Ile, and Leu) can promote collagen synthesis in skin.[31] Our CSCP formulation had appropriately high contents of Leu, Val, Glu, and Ile, indicating potential skin repair effect. Moreover, the CSCPs contained >55mg/g hydrophobic amino acids (Phe, Met, Leu, Val, Ile, Ala, that can remove free ions) and ~20mg/g of aromatic amino acid residues (Tyr, which has a strong antioxidation effect), indicating that the CSCPs have potential antioxidant capacity.[32,33] The combination of the above properties is likely why CSCPs can alleviated UV-induced photo-damage to skin in our model system.

Polypeptides have limitations such as short time of adhesion to skin, poor percutaneous absorption, and easy oxidation during adhesion. This study used a temperature-sensitive gel to overcome these issues. As a porous water-

absorbent material with good biocompatibility, it possesses significant advantages for drug delivery.[27] As one of the few cationic high molecular polymers composed of natural polysaccharides, CS is a useful material to produce temperature-sensitive gels, and its positive charges facilitate electrostatic attraction between the CS and the skin surface, enabling the prepared gel to have closer contact with the skin. Moreover, CS has good bioadhesion and allows the gel to form a film on the skin surface, which increases the adhesion time. The moisturizing property of the CS can effectively improve hydration, making the epidermal cuticle structure swell and loosen with enlarged intercellular space, thus reducing the barrier effect and promoting permeation of the carried drug into the skin.[28,29] CS has good film-forming, adhesive and moisturizing properties. Preparing it into a gel with sustained drug release property can prolong the retention time and increase the drug absorption. CS-based thermosensitive gels have been widely studied as drug delivery materials and used in wound healing, anti-tumor, nasal delivery, and other applications.[54–56] Here we selected CS as the material to prepare temperature-sensitive CS/CSCPs/β-GP gel to enhance its local treatment effect after dermal application. The CS/CSCPs/β-GP gel had a phase transition temperature of 36.3 °C, which is similar to body temperature. After coming into contact with mouse skin, the temperature-sensitive gel rapidly underwent phase transition with a good gelling effect. Macroscopic characterization of mouse skin in the drug administration groups showed that the CS/CSCPs/β-GP gel exhibited more significant anti-SP effects than the CSCPs itself, which corroborated the pathological skin tissue analysis results. These findings indicate that CS/CSCPs/β-GP gel has increased skin adhesion to skin, which prolongs the retention time and increases drug absorption, thus enhancing the therapeutic effect.

It is well known that lower cuticle moisture content and irregular epidermis thickening caused by repeated UV irradiation are direct causes of skin darkness, roughness, and wrinkling.[57,58] Dermal extracellular matrix degradation (especially collagen and elastic fibers) caused by abnormally high MMP expression is the root cause of sagging and wrinkling.[11,59] MMPs are a large family of zinc-dependent endonucleases that play a key role in the over decomposition of extracellular matrix proteins in the dermis.[60] Specifically, MMP-3 can degrade a variety of collagen and elastic fibers, resulting in the typical photoaging appearance of the skin.[38,39] The reticular structure of collagen provides the skin with protection and elasticity, and elastic fibers are the key to keeping the skin elastic and smooth.[37,61] In recent years, many researchers have examined the role genetic metalloproteinase in photoaging.[20,62,63] A previous study reported that CSCPs may exert an anti-photoaging effect by influencing MMPs via the mitogen-activation protein kinase signaling pathway.[20] The observed effects of CSCPs on MMPs found in this study further supports this hypothesis. Notably, we designed a carrier material to magnify the effect of CSCPs, and locally applied this CS/CSCPs/β-GP gel. It effectively inhibited UV-induced abnormal MMP-3 expression and macroscopic and pathologic changes of mouse skin to achieve a good appearance with a relatively smooth, ruddy, and glossy state and only several shallow wrinkles. Collectively, these results suggest that the combination of active substances and gels can be used to treat SP.

Numerous studies have confirmed that UV rays increase ROS to activate NF-κB signaling, which is a central pathway related to cell apoptosis, the inflammatory response, and immune responses in the photoaging process as depicted in Figure 1.[5,6,64] Excessive ROS activates NF-κB to promote the gene transcription of a large number of proinflammatory factors that further promote NF-κB activity. This vicious cycle causes an imbalance between pro- and anti-inflammatory factors in the body, which manifests as continuous proinflammatory response of skin that contributes to the characteristic photoaging appearance.[65] Researchers have demonstrated that TNF-α and IL-1β can stimulate MMP expression and activation, which would further accelerate the degradation of collagen and elastin.[58,66,67] Here, we measured tissue levels of typical proinflammatory factors (TNF-α, IL-1β, and IL-6), one anti-inflammatory factor (IL-10), and ROS. The results showed that UV significantly induced elevated expression of ROS, TNF-α, IL-1β and IL-6 in the skin tissue, but it only promoted IL-10 expression to a certain extent, thus perpetuating an imbalance that led to pathologic responses including inflammatory cell infiltration. After treatment with CS/CSCPs/β-GP gel, proinflammatory factor and ROS levels significantly decreased in mouse skin tissue, while IL-10 levels evidently increased. Based on these findings, we propose that the peptide-carrying gel can reduce proinflammatory factor levels by inhibiting ROS-mediated NF-κB activation. It can also enhance levels of the anti-inflammatory factor IL-10 to restore balance between pro- and anti-inflammatory factors and effectively inhibit skin inflammation. Meanwhile, once NF-κB activation is inhibited, NF-κB-mediated transcription of MMPs (eg, MMP-3) decreases. As a result, there is less degradation of extracellular matrix components such as collagen and elastic fibers. This hypothesis is consistent with the macroscopic characterization and pathological

analysis of skin from the mice in the drug administration group. Moreover, the observation of reduced sagging and fewer thick, deep wrinkles indicate that the gel has good anti-SP effects.

As discussed above, CSCPs themselves contain many hydrophobic amino acids and aromatic amino acid residues that can remove many free ions and exert a strong anti-oxidation effect. Based on this, we infer that the CS/CSCPs/β-GP gel can improve the anti-oxidation capability of skin tissue, inhibit ROS/NF-κB signaling activation and the expression of downstream inflammatory factors, and finally attenuate the photoaging process. This study provides important experimental results for further development in high-value fields such as functional cosmetics for skin aging and anti-photoaging drugs.

Conclusion

The CSCP-based temperature-sensitive gel prepared had a phase transition temperature of 36.3 °C, which is similar to body temperature. After coming into contact with mouse skin, the test substance rapidly underwent phase transition to form a gel with a good gelling effect. According to the CSCP characteristics identified in this study, the molecular weights (concentrated in the range of <2 kDa) showed good potential anti-photoaging effects, and the amino acid composition included many hydrophobic and aromatic amino acid residues that exert strong anti-oxidation effects. Based on this and combined with the macroscopic characterization, pathological sections, and the experimental results of corresponding indicators, we infer that CS/CSCPs/β-GP gel can be applied to prevent the photoaging process. These findings support the further development of CS/CSCPs/β-GP gel in skin aging and related conditions such as abnormal pigmentation (eg, lentigines), benign or malignant tumors such as cutaneous melanoma, and squamous cell carcinoma.

Acknowledgments

Disclosure

The authors declare no conflict of interest.

References

1. Sunder S. Relevant topical skin care products for prevention and treatment of aging skin. *Facial Plast Surg Clin North Am*. 2019;27(3):413–418. doi:10.1016/j.fsc.2019.04.007
2. Leslie B. How to use oral and topical cosmeceuticals to prevent and treat skin aging. *Facial Plast Surg Clin North Am*. 2018;26(4):407–413. doi:10.1016/j.fsc.2018.06.002
3. Simin WU, Yang H. Mechanisms and treatments of skin photoaging by ultraviolet radiation. *Med Recapitulate*. 2018;24(02):341–346. doi:10.3969/j.issn.1006-2084.2018.02.025
4. Aurora G, Mridvika N, Palmira VM, Jaime P, Corinne G. Antiaging effects of a novel facial serum containing L-ascorbic acid, proteoglycans, and proteoglycan-stimulating tripeptide: ex vivo skin explant studies and in vivo clinical studies in women. *Clin Cosmet Investig Dermatol*. 2018;11:253–263. doi:10.2147/CCID.S161352
5. Subedi L, Lee TH, Wahedi HM, Baek S-H, Kim SY. Resveratrol-enriched rice attenuates UVB-ROS-induced skin aging via downregulation of inflammatory cascades. *Oxid Med Cell Longev*. 2017;2017:8379539. doi:10.1155/2017/8379539
6. He L, Lin X, Chen H, Sui C, Li M, Zhu W. Research progress in the mechanisms and therapeutic agents of skin photoaging. *J Pract Dermatol*. 2010;13(5):293–296. doi:10.11786/sypfbxzz.1674-1293.20200510
7. Herrling T, Jung K, Fuchs J. Measurements of UV-generated free radicals/reactive oxygen species (ROS) in skin. *Spectrochim Acta A Mol Biomol Spectrosc*. 2006;63(4):840–845. doi:10.1016/j.saa.2005.10.013
8. Jenkins G. Molecular mechanisms of skin ageing. *Mech Ageing Dev*. 2002;123(7):801–810. doi:10.1016/S0047-6374(01)00425-0
9. Girsang E, Ginting CN, Lister INE, Gunawan KY, Widowati W. Anti-inflammatory and antiaging properties of chlorogenic acid on UV-induced fibroblast cell. *PeerJ*. 2021;9:e11419. doi:10.7717/peerj.11419
10. Pittayapruek P, Meephansan J, Prapapan O, Komine M, Ohtsuki M. Role of matrix metalloproteinases in photoaging and photocarcinogenesis. *Int J Mol Sci*. 2016;17(6):868. doi:10.3390/ijms17060868
11. Zeng L, Hu H, Xie H, Chen N, Li M, Deng Y. Research progress of skin photoaging. *Med Sci J Central South China*. 2015;43(2):226–229. doi:10.15972/j.cnki.43-1509/r.2015.02.029
12. Ai L. *Study on Protective Effect of Cod Skin Collagen Peptides Against Skin Photoaging and Its Action Mechanism*. South China University of Technology. 2020.
13. Liang F, Zuo H. A review of the properties, applications and development prospects of collagen peptide. *Sci Technol Gelatin*. 2014;34(03):109–115.

14. Hou H, Zhao X, Li B, Zhang Z, Zhuang Y. Inhibition of melanogenic activity by gelatin and polypeptides from pacific cod skin in B16 melanoma cells. *J Food Biochem*. 2011;35(4):1099–1116. doi:10.1111/j.1745-4514.2010.00437.x

15. Li X. *Study on the Water Retention and Skin Care of Cod Skin Collagen Peptide*. Ocean University of China; 2014.

16. Liu C, Zhao Y, Yang Z, Ding G. Protective effect of cod skin collagen peptides on acute liver injury in mice. *Modern Food Sci Technol*. 2015;31 (7):18–24. doi:10.13982/j.mfst.1673-9078.2015.7.004

17. Wang J, Liu C, Ding G, Zheng Y, Zhao Y, Yang Z. Effect of cod skin collagen peptide on chronic liver injury induced by carbon tetrachl oride in mice. *Acta Nutrimenta Sinica*. 2016;38(2):133–137. doi:10.13325/j.cnki.acta.nutr.sin.2016.02.009

18. Wang Z, Sun J, Ni X, Hou H, Bao Y, Li B. Anti-alcoholic gastric ulcer effect of collagen peptide extracted from skin of walleye pollock. *Chin J Marine Drugs*. 2012;31(5):17–22. doi:10.13400/j.cnki.cjmd.2012.05.006

19. Zhang J. Preparation of peptides by probiotic fermentation from cod skin and its antioxidant properties in vitro. *Yantai Univ*. 2012. doi:10.7666/d. D373372

20. Chen TJ, Hou H, Fan Y, et al. Protective effect of gelatin peptides from pacific cod skin against photoaging by inhibiting the expression of MMPs via MAPK signaling pathway. *J Photochem Photobiol B*. 2016;165:34–41. doi:10.1016/j.jphotobiol.2016.10.015

21. Zhang Y, Xu HW, Han YT, et al. Aquaporin 3 contributes to cytoprotective effect of collagen peptides from walleye pollock skin against hydrogen peroxide induced oxidative stress damage in HaCaT cells. *Chin J Pharmacol Toxicol*. 2015;893–898. doi:10.3867/j.issn.1000-3002.2015.06.003

22. Wang X, Ren L, Qiang T, Zhou G, Li F. Research progress of collagen and its application in cosmetics. *China Surfactant Detergent Cosmet*. 2005;35(06):388–392. doi:10.13218/j.cnki.csdc.2005.06.013

23. Zheng B, Ruan G, Zhang S, et al. A new method for establishing animal model of rapid photoaging. *Dermatol Venereol*. 2017;39(04):241–244. doi:10.3969/j.issn.1002-1310.2017.04.003

24. Li Z, Niu X, Xiao S, et al. Improvement of establishing skin photoaging model in mice. *J Xi'an Jiaotong Univ*. 2016;37(1):144–147+156. doi:10.7652/jdyxb201601028

25. Battie C, Jitsukawa S, Bernerd F, Del Bino S, Marionnet C, Verschoore M. New insights in photoaging, UVA induced damage and skin types. *Exp Dermatol*. 2014;23:7–12. doi:10.1111/exd.12388

26. Gilhar A, Etzioni A. The nude mouse model for the study of human skin disorders. *Dermatology*. 1994;189(1):5–8. doi:10.1159/000246750

27. Kang X, Deng A, Yang S. Research progress of chitosan based thermosensitive hydrogels. *China Biotechnol*. 2018;38(5):79–84. doi:10.13523/j. cb.20180511

28. Nair R, Reddy BH, Kumar CKA, Kumar KJR. Application of Chitosan microspheres as drug carriers: a review. *J Pharm Sci*. 2009;17:1–12.

29. Yenilmez E, Başaran E, Yazan Y, et al. Release characteristics of vitamin E incorporated chitosan microspheres and in vitro– in vivo evaluation for topical application. *Carbohydr Polym*. 2011;84(2):807–811. doi:10.1016/j.carbpol.2010.07.002

30. Do-Un K, Hee-Chul C, Jia C, Yasuo S, Boo-Yong L. Oral intake of low-molecular-weight collagen peptide improves hydration, elasticity, and wrinkling in human skin: a randomized, double-blind, placebo-controlled study. *Nutrients*. 2018;10(7):826. doi:10.3390/nu10070826

31. Li C, Fu Y, Dai H, Wang Q, Gao R, Zhang Y. Recent progress in preventive effect of collagen peptides on photoaging skin and action mechanism. *Food Sci Hum Well*. 2022;11(2):12. doi:10.1016/j.fshw.2021.11.003

32. Harnedy PA, Fitzgerald RJ. Bioactive peptides from marine processing waste and shellfish: a review. *J Funct Foods*. 2012;4(1):6–24. doi:10.1016/j. jff.2011.09.001

33. Kumar N, Nazeer RA, Jaiganesh R. Purification and biochemical characterization of antioxidant peptide from horse mackerel (Magalaspis cordyla) viscera protein. *Peptides*. 2011;32(7):1496–1501. doi:10.1016/j.peptides.2011.05.020

34. Wang T, Chen L, Shen T, Wu D. Preparation and properties of a novel thermo-sensitive hydrogel based on chitosan/hydroxypropyl methylcellulose/ glycerol. *Int J Biol Macromol*. 2016;93(Pt A):775–782. doi:10.1016/j.ijbiomac.2016.09.038

35. Kong S-Z, Chen H-M, Yu X-T, et al. The protective effect of 18β-Glycyrrhetinic acid against UV irradiation induced photoaging in mice. *Exp Gerontol*. 2015;61:147–155. doi:10.1016/j.exger.2014.12.008

36. Bissett DL, Chatterjee R, Hannon DP. Photoprotective effect of topical anti-inflammatory agents against ultraviolet radiation-induced chronic skin damage in the hairless mouse. *Photodermatol Photoimmunol Photomed*. 1990;7(4):153–158. doi:10.1016/0190-9622(90)70232-7

37. Chung JH. Photoaging in Asians. *Photodermatol Photo*. 2010;19(3):109–121. doi:10.1034/j.1600-0781.2003.00027.x

38. Brenneisen P, Sies H, Scharffetter-Kochanek K. Ultraviolet-B irradiation and matrix metalloproteinases: from induction via signaling to initial events. *Ann NY Acad*. 2002;973:31–43. doi:10.1111/j.1749-6632.2002.tb04602.x

39. Zheng J, Lu C, Wei L. Matrix metalloproteinases and skin photoaging. *Chin J Med Aesthetics Cosmetol*. 2012;18(1):75–77. doi:10.3760/cma.j. issn.1671-0290.2012.01.027

40. Keshari S, Balasubramaniam A, Myagmardoloonjin B, Herr DR, Negari IP, Huang CM. Butyric acid from probiotic Staphylococcus epidermidis in the skin microbiome down-regulates the ultraviolet-induced pro-inflammatory IL-6 cytokine via short-chain fatty acid receptor. *Int J Mol Sci*. 2019;20(18):4477. doi:10.3390/ijms20184477

41. Lin TY, Wu PY, Hou CW, et al. Protective effects of sesamin against UVB-induced skin inflammation and photodamage in vitro and in vivo. *Biomolecules*. 2019;9(9):479. doi:10.3390/biom9090479

42. Scharffetter-Kochanek K, Wlaschek M, Brenneisen P, Schauen M, Wenk J. UV-induced reactive oxygen species in photocarcinogenesis and photoaging. *Biol Chem*. 2001;378(11):1247–1257. doi:10.1089/ars.2005.7.1423

43. Johnston KJ, Oikarinen AI, Lowe NJ, Clark JG, Uitto J. Ultraviolet radiation-induced connective tissue changes in the skin of hairless mice. *J Invest Dermatol*. 1984;82(6):587–590. doi:10.1111/1523-1747.ep12261342

44. Chen XY, Ma WY Protective effect and mechanism of water extract of hippophae rhamnoides on HaCaT cells injured by UVC radiation. *Shandong Medical Journal*. 2017;57(13):42–44. doi:10.3969/j.issn.1002-266X.2017.13.012

45. Hironobu I, Tetsuya O. The Mechanisms of UV Mutagenesis. *J Radiat Res*. 2011;52(2):115–125. doi:10.1269/jrr.10175

46. Silveira JE, Pedroso DMM. UV light and skin aging. *Rev Environ Health*. 2014;29(3):243–254. doi:10.1515/reveh-2014-0058

47. Chen T, Hou H, Lu J, Zhang K, Li B. Protective effect of gelatin and gelatin hydrolysate from salmon skin on UV irradiation-induced photoaging of mice skin. *J Ocean Univ China*. 2016;15(4):711–718. doi:10.1007/s11802-016-2953-5

48. Iosageanu A, Ilie D, Craciunescu O, et al. Effect of fish bone bioactive peptides on oxidative, inflammatory and pigmentation processes triggered by UVB irradiation in skin cells. *Molecules*. 2021;26(9):2691. doi:10.3390/molecules26092691

49. Xiao Z, Liang P, Chen J, et al. A peptide YGDEY from tilapia gelatin hydrolysates inhibits UVB-mediated skin photoaging by regulating MMP-1 and MMP-9 expression in HaCaT cells. *Photochem Photobiol*. 2019;95(6):1424–1432. doi:10.1111/php.13135

50. Zhang S-Y, Zhao Y-Q, Wang Y-M, Yang X-R, Chi C-F, Wang B. Gelatins and antioxidant peptides from Skipjack tuna (Katsuwonus pelamis) skins: purification, characterization, and cytoprotection on ultraviolet-A injured human skin fibroblasts. *Food Biosci*. 2022;102138. doi:10.1016/j. fbio.2022.102138

51. Lee H-J, Jang H-L, Ahn D-K, et al. Orally administered collagen peptide protects against UVB-induced skin aging through the absorption of dipeptide forms, Gly-Pro and Pro-Hyp. *Biosci Biotechnol Biochem*. 2019;83(6):1146–1156. doi:10.1080/09168451.2019.1580559

52. Chen T, Hou H. Protective effect of gelatin polypeptides from Pacific cod (Gadus macrocephalus) against UV irradiation-induced damages by inhibiting inflammation and improving transforming growth Factor-β/Smad signaling pathway. *J Photochem Photobiol B*. 2016;162:633–640. doi:10.1016/j.jphotobiol.2016.07.038

53. Kim D, Lee M, Yang JH, Yang JS, Kim O-K. Dual skin-whitening and anti-wrinkle function of low-molecular-weight fish collagen. *J Med Food*. 2022;25(2):192–204. doi:10.1089/jmf.2021.K.0124

54. Dong X, Yao F, Jiang L, et al. Facile preparation of a thermosensitive and antibiofouling physically crosslinked hydrogel/powder for wound healing. *J Mater Chem B*. 2022;10(13):2215–2229. doi:10.1039/D2TB00027J

55. Nkanga CI, Steinmetz NF. Injectable hydrogel containing cowpea mosaic virus nanoparticles prevents colon cancer growth. *ACS Biomater Sci Eng*. 2022;8(6):2518–2525. doi:10.1021/acsbiomaterials.2c00284

56. Alami-Milani M, Salatin S, Rayeni FS, Jelvehgari M. Preparation and in vitro evaluation of thermosensitive and mucoadhesive hydrogels for intranasal delivery of phenobarbital sodium. *Ther Deliv*. 2021;12(6):461–475. doi:10.4155/tde-2021-0022

57. Jung JW, Cha SH, Lee SC, Chun IK, Kim YP. Age-related changes of water content in the rat skin. *J Dermatol Sci*. 1997;14(1):12–19. doi:10.1016/S0923-1811(96)00542-7

58. Misawa E, Tanaka M, Saito M, et al. Protective effects of Aloe sterols against UVB-induced photoaging in hairless mice. *Photodermatol Photo*. 2017;33(2):101–111. doi:10.1111/phpp.12286

59. Jung YY, Ha IJ, Lee M, Ahn KS. Skin Improvement with Antioxidant Effect of Yuja (Citrus junos) Peel Fractions: Wrinkles, Moisturizing, and Whitening. *Antioxidants*. 2022;12(1):51 doi:10.3390/antiox12010051.

60. Quan T, Qin Z, Xia W, Shao Y, Voorhees JJ, Fisher GJ. Matrix-degrading metalloproteinases in photoaging. *Elsevier*. 2009;20–24. doi:10.1038/jidsymp.2009.8

61. Fisher GJ, Wang Z, Datta SC, Varani J, Kang S, Voorhees JJ. Pathophysiology of premature skin aging induced by ultraviolet light. *N Engl J Med*. 1997;337(20):1419–1429. doi:10.1056/NEJM199711133372003

62. Li Y, Xia C, Yao G, et al. Protective effects of liquiritin on UVB-induced skin damage in SD rats. *Int Immunopharmacol*. 2021;97:107614. doi:10.1016/j.intimp.2021.107614

63. Auh J-H, Madhavan J. Protective effect of a mixture of marigold and rosemary extracts on UV-induced photoaging in mice. *Biomed Pharmacother*. 2021;135:111178. doi:10.1016/j.biopha.2020.111178

64. Wang SH, Chen YS, Lai KH, et al. Prinsepiae Nux extract activates NRF2 activity and protects UVB-induced damage in keratinocyte. *Antioxidants*. 2022;11(9 1755). doi:10.3390/antiox11091755

65. Saito P, Melo C, Martinez RM, Fattori V, Casagrande R. The lipid mediator resolvin D1 reduces the skin inflammation and oxidative stress induced by UV irradiation in hairless mice. *Front Pharmacol*. 2018;9:1242. doi:10.3389/fphar.2018.01242

66. Vaalamo M, Mattila L, Johansson N, et al. Distinct populations of stromal cells express collagenase-3 (MMP-13) and collagenase-1 (MMP-1) in chronic ulcers but not in normally healing wounds. *J Invest Dermatol*. 1997;109(1):96–101. doi:10.1111/1523-1747.ep12276722

67. Taddese S, Jung MC, Ihling C, Heinz A, Neubert RHH, Schmelzer CEH. MMP-12 catalytic domain recognizes and cleaves at multiple sites in human skin collagen type I and type III. *Biochim Biophys Acta Proteins Proteom*. 2010;1804(4):731–739. doi:10.1016/j.bbapap.2009.11.014